Large or Small Iris Aperture in SC multicell cavities ?

E. Haebel
CERN, Geneva, Switzerland

A. Mosnier
Centre d'Etudes de Saclay, France

1. Introduction

As the cost of the superconducting linear accelerator, which could be used for future TeV linear colliders [1], is dominated by the accelerating structure, every effort has to be made to reduce structure cost and increase gradients beyond the level that has been reliably obtained today. Accordingly, the cavity design is of outstanding importance. For that purpose, an ideal structure should meet the four fundamental requirements :

- the number of cells should be high to reduce structure cost
- the peak surface electrical field should be low as field emission is the dominant gradient limitation to date
- the higher order modes should be properly damped to avoid multibunch instabilities
- the dissipated power in the low temperature helium bath should be as low as possible

Bearing a large number of cells per cavity in mind, this paper emphasizes the choice of the cell iris opening. The overall performances (gradient, damping efficiency, heat load) of two 9-cell structures, with the same basic cell shape, but with small and large iris apertures, are compared and discussed.
In the following, a cavity frequency of 1500 MHz has been chosen, but a scaling is obviously possible.

2. The fundamental mode problem

The admitted cell geometry, which gives the lower peak surface electric E_{pk} is the elliptic shape in the iris region. A round shape in the equator region gives a lower magnetic field B_{pk} . While a reduced shunt impedance r/Q increases the dissipated power at the cryogenic temperature, the peak surface electric field governs the final gradient, which is usually limited by field emission. Figures 1 shows the results of single cell π-mode calculations with the cavity code Urmel [2] when the iris opening is varied. The classical small iris curvature radius (6 mm) has been kept because a larger radius can lead to some dangerous trapped modes as a result of destructive mode mixing [3].
We see that r/Q and B_{pk} vary about linearly with the iris aperture and that E_{pk} behaves like a S-curve. From the surface electric field point of view, an iris aperture around 28 mm should be a good choice as the gain becomes minor with smaller aperture. If we choose a first cavity with 28 mm and a second one with 40 mm iris aperture, the situation is summarized in table 1. The cell to cell coupling for the small iris is 1.4 % and seems still reasonable.

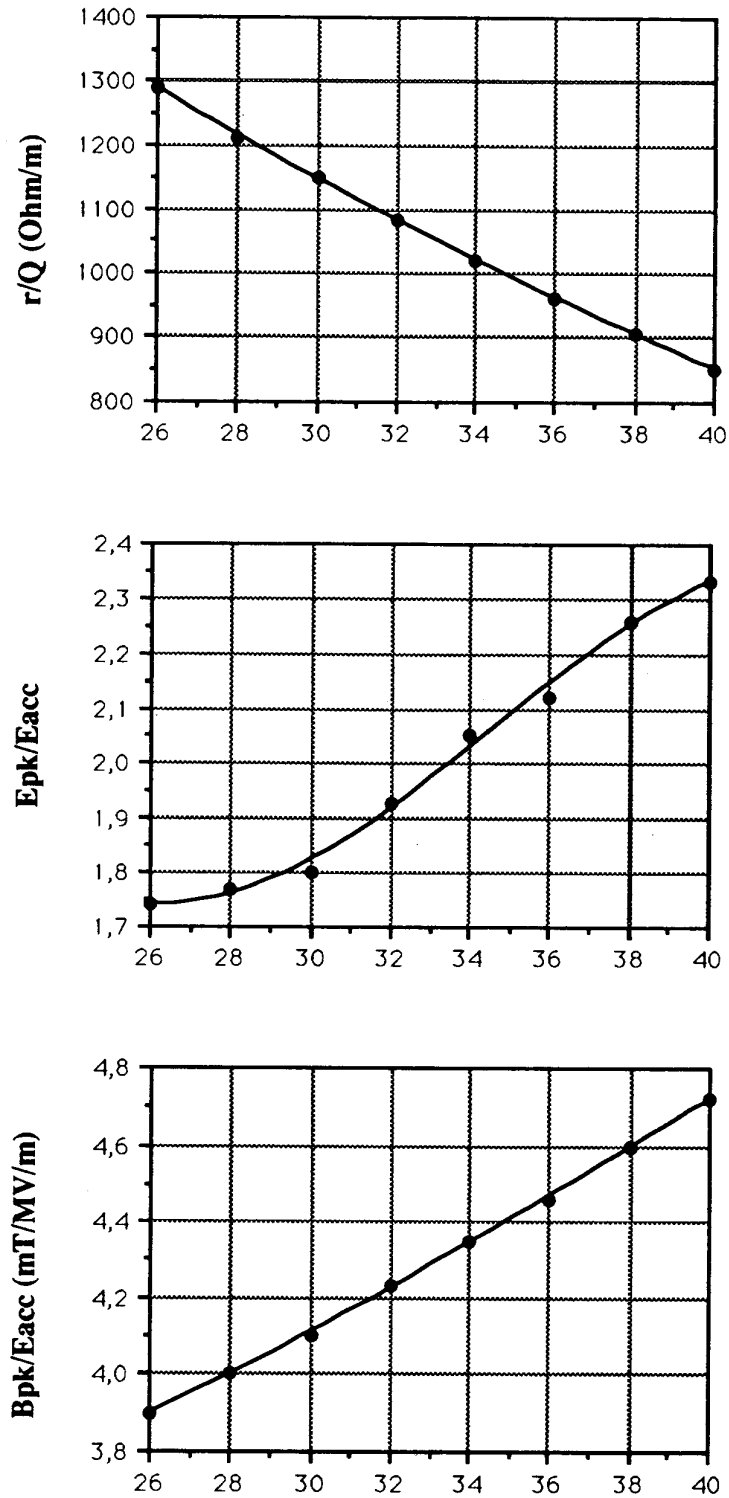

Figure 1 : Impedance shunt, peak surface electric and magnetic fields for different iris openings (mm).

Iris aperture	r/Q (Ohm/m)	E_{pk}	B_{pk} (mT/MV/m)
40 mm	850	2.6	4.9
28 mm	1200	1.8	4.0
Gain	41 %	44 %	22 %

Table 1 : Impedance shunt, peak surface electric and magnetic fields for different iris openings

If we consider a pulsed superconducting linac with an effective cryogenic duty factor of 1.4 %, cavities achieving a gradient of 25 MV/m with a Q_0 of 10^{10} , the cavity dissipation in the helium bath will be about 0.7 and 1.0 Watts per active length for respectively 28 and 40 mm iris aperture.
The resulting two 9-cell structures with small (cavity 28 and cavity 40) and large iris aperture and elliptic shape in the iris region which we intend to compare are sketched in Figures 2 and 3. The tuning of the half end cell for a flat fundamental mode has been obtained with the help of a slightly larger outer beam tube radius (33 mm) for the cavity of small iris aperture and of a larger slope in the straight segment for the large iris aperture. The outer beam tube cannot be larger than 40 mm because the fields would penetrate too much and could degrade the filling factor defined by the active structure length over total length ratio.

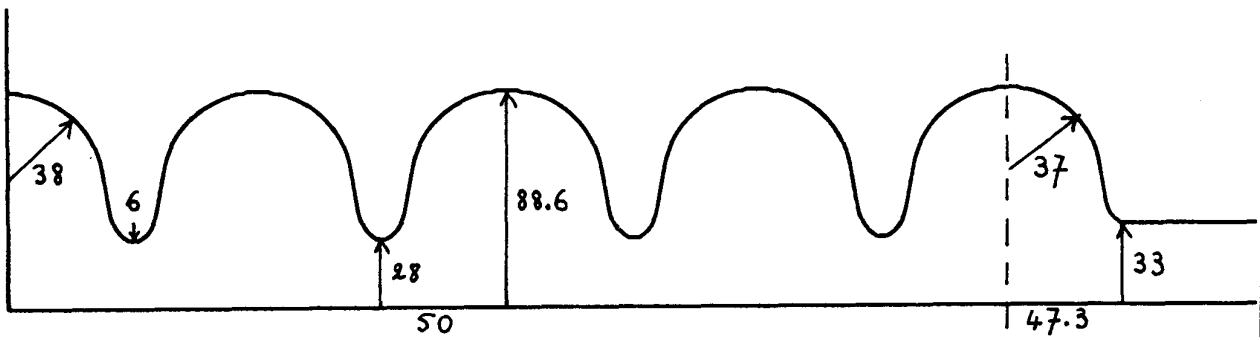

Figure 2 : Cavity 28 (9-cell cavity with 28 mm iris apertute)

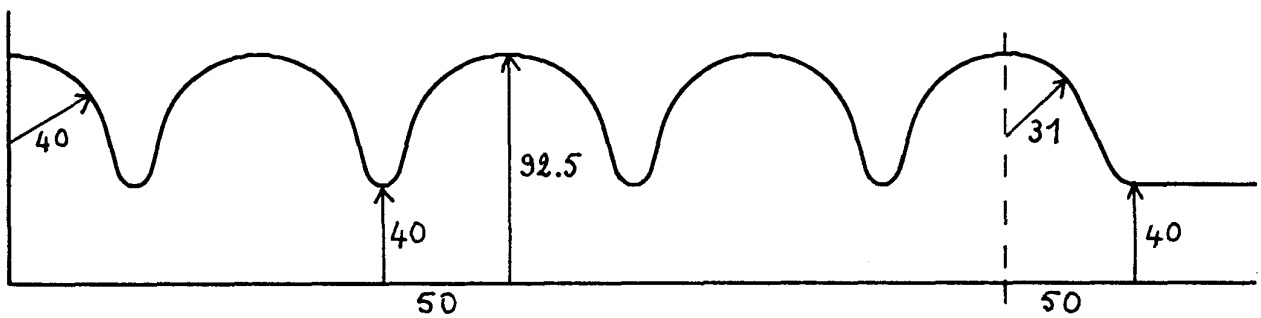

Figure 3 : Cavity 40 (9-cell cavity with 40 mm iris apertute)

3. The loss factor problem

The evaluation of energy deposition by the beam into the cavities is of great importance since part of the resulting power can be dissipated at cryogenic temperature. In addition, some bunch energy spread is induced by the variation of the wakefield across the bunch. The power deposited by the beam is given by $P_{HOM} = k_{HOM}\, q^2\, f_r$ where q is the bunch charge, f_r is the average bunch repetition rate and k is the loss factor. Time domain cavity codes like TBCI [4] can be used to compute the total loss parameter k_{tot}. The fundamental mode loss parameter k_{fund} has then to be subtracted

$$k_{HOM} = k_{tot} - k_{fund} \qquad \text{with} \quad k_{fund} = \frac{\omega}{4} R/Q\, e^{-\omega^2 \sigma_t^2} \qquad \text{for gaussian bunches.}$$

However, since numerical codes require that the bunch spectrum does not extend too much above the critical uppermesh frequency, the mesh size has to be less than 0.2 mm for a bunchlength of σ_z = 1 mm. TBCI requires square meshes so that for a 9-cell cavity, the number of mesh points required should be greater than 2.25 millions for TBCI whereas a maximum of 400000 mesh points is allowed on the CRAY2 computer we used. Fortunatly, the code ABCI [5] permits unequal mesh sizes in the axial and radial directions and then short bunch wake potentials in long structures could be computed. The mesh size was fixed to 1.8 in radial and 0.18 mm in axial direction. Figures 4 and 5 show the total loss factors per cavity in V/pC for the two 9-cell structures with 40 and 28 mm iris aperture. We consider the cavity alone (full circles) or with a beam tube reduction (reduced tube radius 21 mm) at a distance of 65 mm of the last iris. The reason of the beam tube shrinkening will be given hereafter. We note that, on a short range, the loss factor scales as $\sigma_z^{-1/2}$ as expected [6]. However, the two iris diameters being too much different, the scaling with the iris radius is not linear. Table 2 which resumes the situation for a bunchlength of 1 mm shows the clear advantage of the cavity with large iris and without beam tube enlargement.

Iris aperture	k fund (V/pc/m)	k_{HOM} (V/pC/m) without reduction	k_{HOM} (V/pC/m) with reduction
40 mm	2.0	7.6	11.8
28 mm	2.8	12.9	15.2

Table 2 : HOM loss factor per active length for the two structures without and with beam tube reduction (bunchlength = 1 mm).

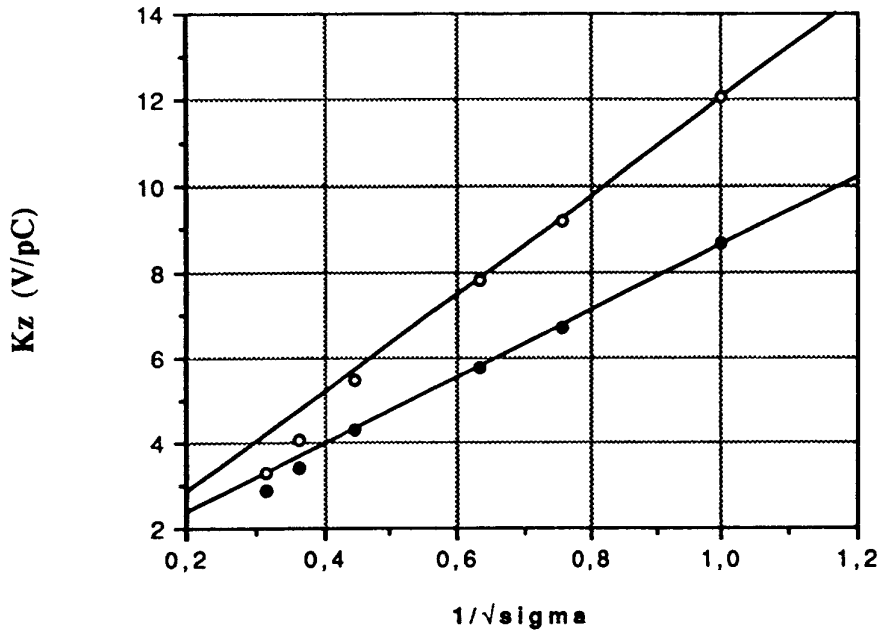

Figure 4 : total loss factor of a 9-cell structure with 40 mm iris aperture for different bunchlengthes without (full circles) and with beam tube reduction (empty circles)

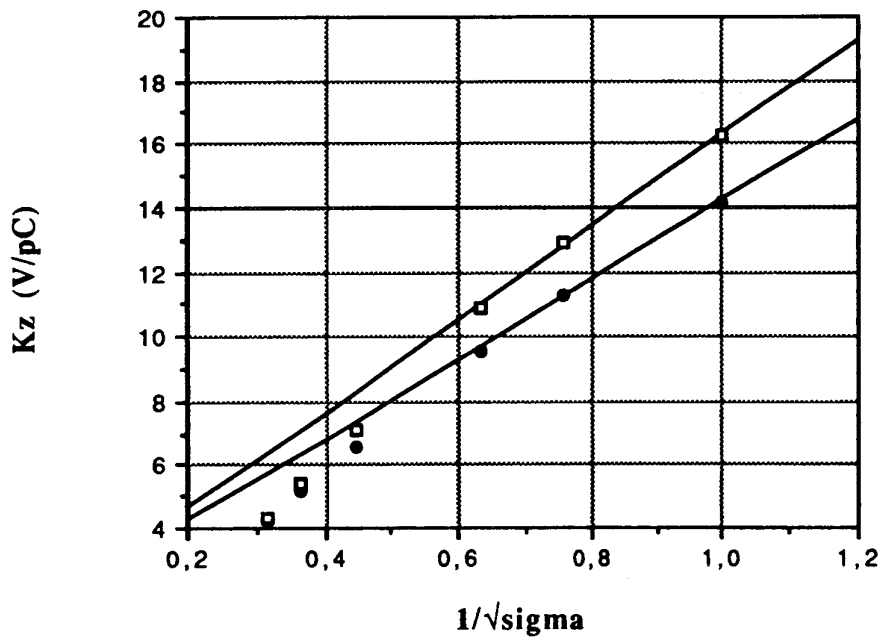

Figure 5 : total loss factor of a 9-cell structure with 28 mm iris aperture for different bunchlengthes without (full circles) and with beam tube reduction (empty circles)

4. The HOM damping problem

High Q parasitic modes can destabilize the train of bunches passing through the accelerating structures. For limiting both transient longitudinal and transverse emittances, external couplers must then be mounted on the beam tubes of each cavity to damp the higher order modes. Calculations on the maximum tolerable Qs are going on (see for example [7]) but we assume at present that the Q for both the longitudinal and transverse modes of high R/Q has to be reduced to a level between 10^5 and 10^6.

The non propagating modes

First we analyse the non propagating modes. The TM011 mode at about twice the fundamental mode frequency is the most dangerous longitudinal mode because of its high R/Q. Following the end-cell compensation method used in [8], the external curvature radius of the last half cell was varied to over compensate the TM011- π mode while the length was adjusted to keep the accelerating TM010- π mode flat. Figure 6 shows for example the growing radial electric field from the middle cell to the outer cell after optimization of the cavity with 28 mm iris radius.

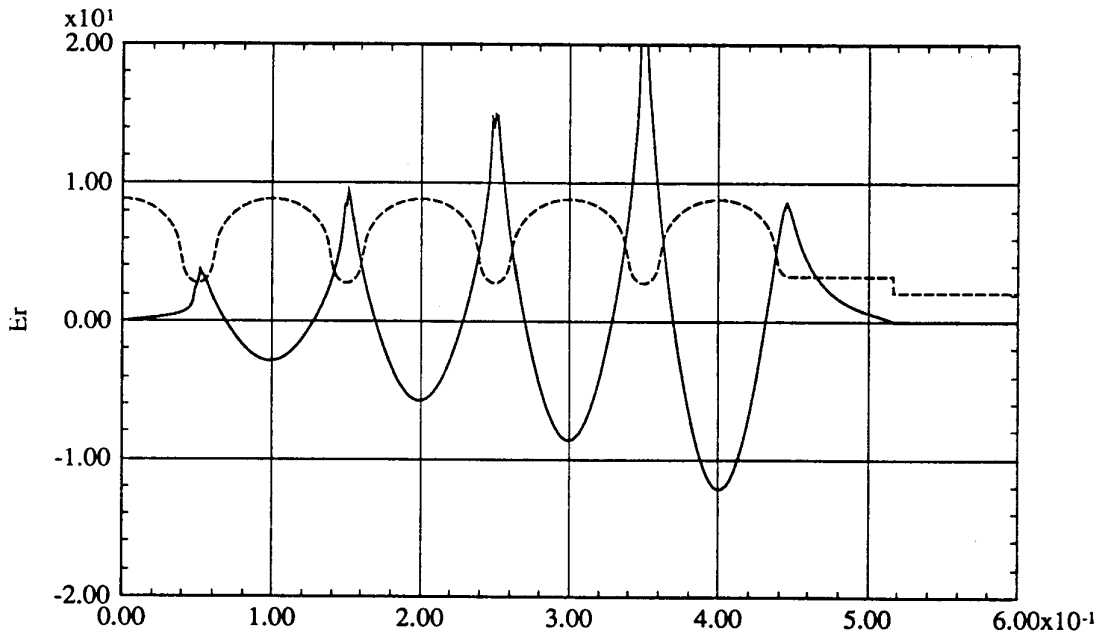

Figure 6 : Radial electric field at 28 mm from the axis along the small iris cavity fot the TM011- π mode (2783 MHz) after compensation.

For dipole modes, the TM110 modes are usually more difficult to damp than the TE111-ones because they don't penetrate deeply into the beam tube. But finally on the whole, the damping is found very similar to the case of cavities with a smaller number of cells. However, as the first dipole modes start at frequencies very close to the fundamental mode in the case of the large iris cavity, the HOM coupler must be carefully designed. Knowing the field levels at the coupler location and assuming that monopole modes are damped with an antenna and dipole modes with a loop, the anticipated external Q were deduced according to the classical formulae :

$$Q\,ex = \frac{\omega U}{P_{dis}} \quad \text{with} \quad P_{dis} = \frac{1}{2} R I^2 \quad \text{or} \quad P_{dis} = \frac{1}{2} \frac{V^2}{R}$$

where V is the induced voltage on the loop, I is the picked up displacement current on the probe, U is the stored energy and R is the resistive load

After numerous computations with Urmel, we concluded that for the highest R/Q modes, the Qs of the cavity 28 are about 2 times greater than those of the cavity 40.Tables 3 and 4 give for instance the highest coupling impedances (Ω/m for monopole and Ω/m^3 for dipole modes) per active length for both structures.

Cavity 28		Cavity 40	
R/Q	Qex (10^6)	R/Q	Qex (10^6)
107	2,3	56	1,7
53	4,0	41	2,0
29	3,4	22	3,5
8	5,1	17	3,5

Table 3 : Calculated Qex for the highest R/Q TM011-like modes.

Cavity 28		Cavity 40	
R/Q (10^4)	Qex (10^4)	R/Q (10^4)	Qex (10^4)
8,5	3,5	4,5	2,1
5,3	2,2	2,7	3,5
2,7	5,8	1,5	1,3
0,9	1,0	1,4	0,2

Table 4 : Calculated Qex for the highest R/Q TM110-like modes.

In addition we note that, as usual, the coupling system should have an enhancement of about 10 dB in the transmission response around the TM011 passband, which will reduce the quoted TM011 mode Qex values by a factor 10.

The propagating modes

Among these modes, we find unfortunatly several trapped modes which, although above cut-off, couple very poorly to the beam tube. But we have to worry only about those with higher R/Q. The two troublesome families are the TM012-like for the monopole and the TE121-like (fifth passband) for the dipole modes. Figure 7 shows for example the radial electric field along the small iris cavity for a rather high R/Q mode (about 20 Ω/m) in the TM012 passband. In the same way, figure 8 shows the axial magnetic field of a mode in the fifth dipole passband, which has a small but non

negligible impedance (R/Q = 1,5 10^3 Ω/m^3) . Note that this field crosses zero just at the coupling port.

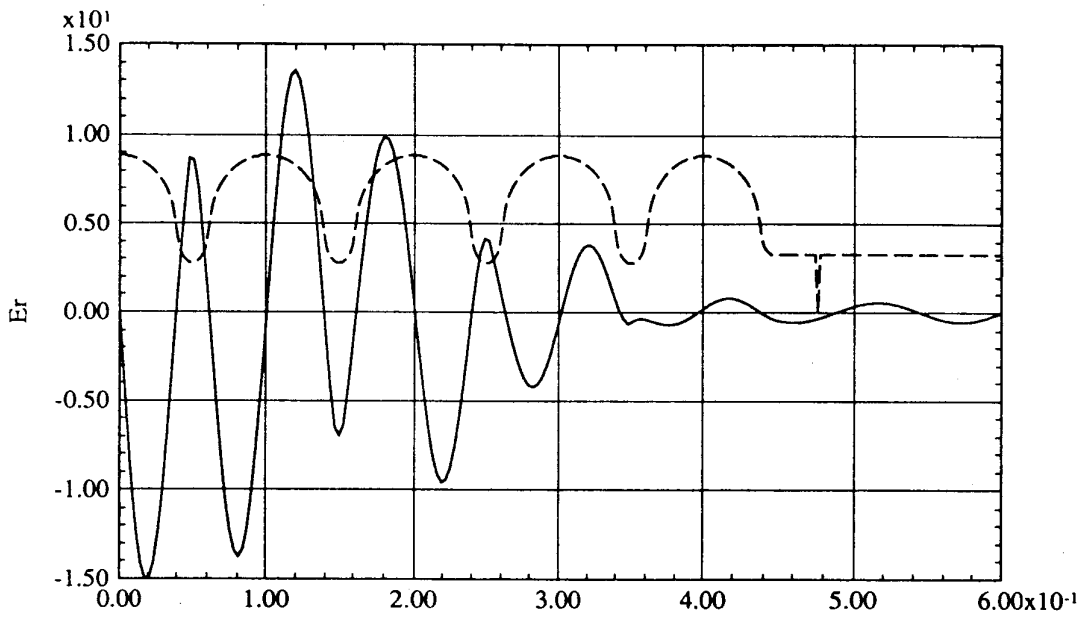

Figure 7 : radial electric field at 25mm from the beam axis along the cavity 28 for the highest R/Q TM012-like mode.

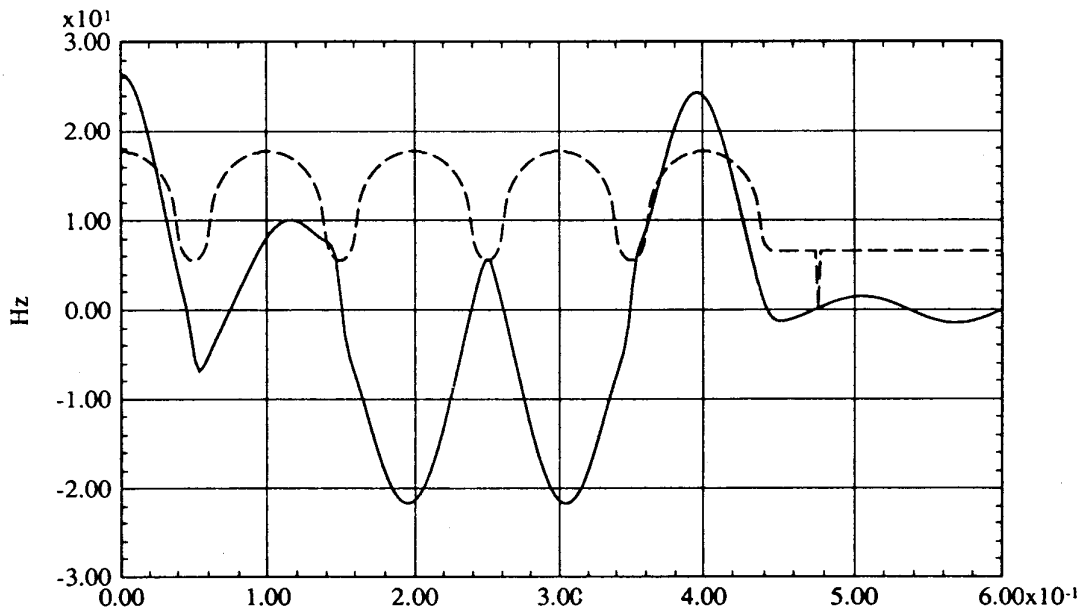

Figure 8 : axial magnetic field at 25 mm from the beam axis along the cavity 28 for the highest R/Q TE121-like mode.

Both structures present these two trapped families at about the same frequency : around 4300 MHz for TM012 and 3500 MHz for TE121. Some modes of the fifth dipole passband have no field at all in the beam tube but these modes have fortunatly a very low R/Q and we assume that they will not have a significant effect on the multibunch instabilities. We have hence to worry only about two modes both in the longitudinal TM012 passband and in the fifth dipole passband. To get rid of these annoying trapped modes, the following remedies can be prospected :
A first method, described in [8], makes use of a beam tube reduction to cut off the propagation of the TM012 and TE121 waves. The diameter reduction can have two beneficial effects if the position is judiously chosen : the excitation of the end cells and hence the coupling field in the beam tube is enhanced and the maximum field of the standing wave pattern is fixed just at the coupler location. Figure 9 shows the field level within the wider part of the beam tube for different reduction positions. The optimum location for the TM012 (≥70mm) does not correspond to the optimum location for the TE121 (≤60mm), so that a compromise has to be chosen. Once the adjustment of the beam tube reduction has been made, the resulting impedances (R/Q Qex) are found to be slightly lower than the impedances of the highest R/Q non propagating modes. Although this method is very efficient, the main drawback is an increase of beam induced power as the beam tube reduction behaves like a step for the beam. As the frequencies of the modes in question are about the same for both structures, the reduced beam tube radius must be the same for both cavity versions and smaller than 25 mm. From table 2 we read a loss factor increment of about 18 % for the small iris cavity and 55 % for the large iris cavity.

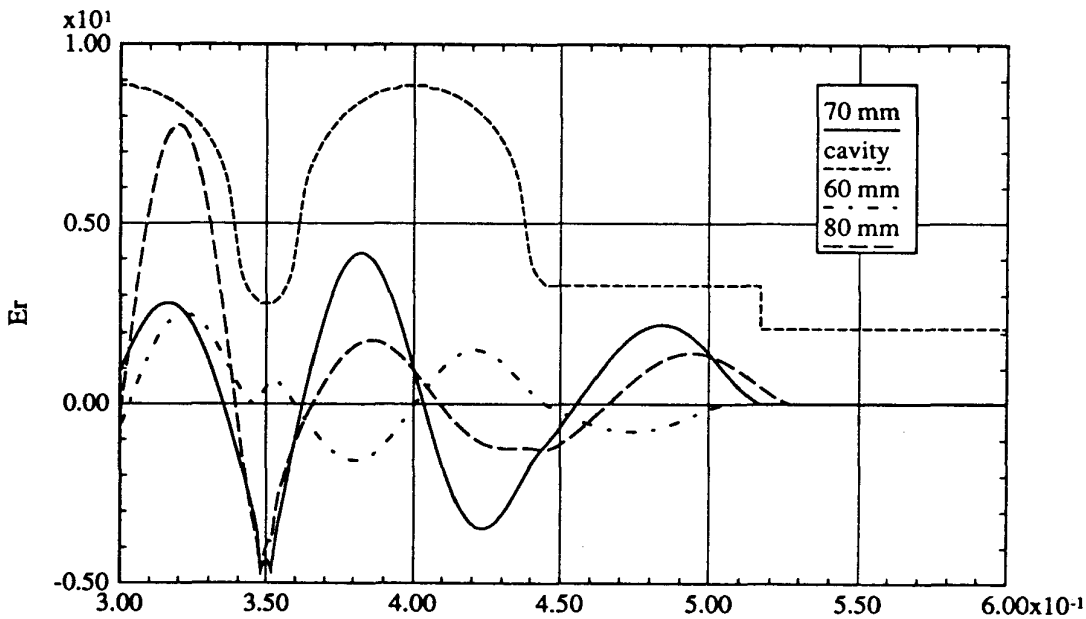

Figure 9 : radial electric field of the TM012-like mode at 35mm from the beam axis at the end of the cavity 28 for different locations of the beam pipe reduction.

Without beam tube reduction, it is essential that the HOM couplers sit near to the peak of the weakened standing wave pattern of the trapped modes. Combining 8 cavities in one module means for frequencies above cut-off that one assembles a multiperiodic structure with at least 8 times more "supermodes" than the individual 9-cell cavity. For each of these supermodes we have a standing wave pattern in the beam tubes between cavities with the inherent risk that couplers sit near to a field zero, rendering them ineffective. For non trapped modes, the HOM power is evacuated both by end beam

tubes and by the couplers because not all of the 16 available couplers will see field zeros. However for trapped modes, as the cavity to cavity coupling is very small (less than 10^{-4}), the always present cavity frequency perturbations due to mechanical tolerances will easily destroy the weakly coupled supermodes such that the cavities behave again as individual resonators. By varying the distance between two cavities, the position of the field zeros changes but Urmel calculations predict that these positions do practically not move with moderate frequency perturbations. However if the distance between two adjacent cavities corresponds to 3 half wavelengths, the zero crossing of the electric field for the TM012 mode is 3 cm away from the last iris, which is unfortunatly the optimal coupler location for the non propagating modes. Figure 10 and 11 show for instance the radial electric field for the TM012 mode along two 9-cell cavities, while the second cavity is slightly detuned, respectively 3 half wavelengths and 3 half wavelengths plus 4 cm away from one another. The optimized distance between two adjacent cavities for both TM012 and TE121 modes is found to be about 3 half wavelengths plus 4 or 6 cm. In this case, the beam tube reduction could be avoided but measurements on copper prototypes with at least 2 cavities are needed to confirm this solution.

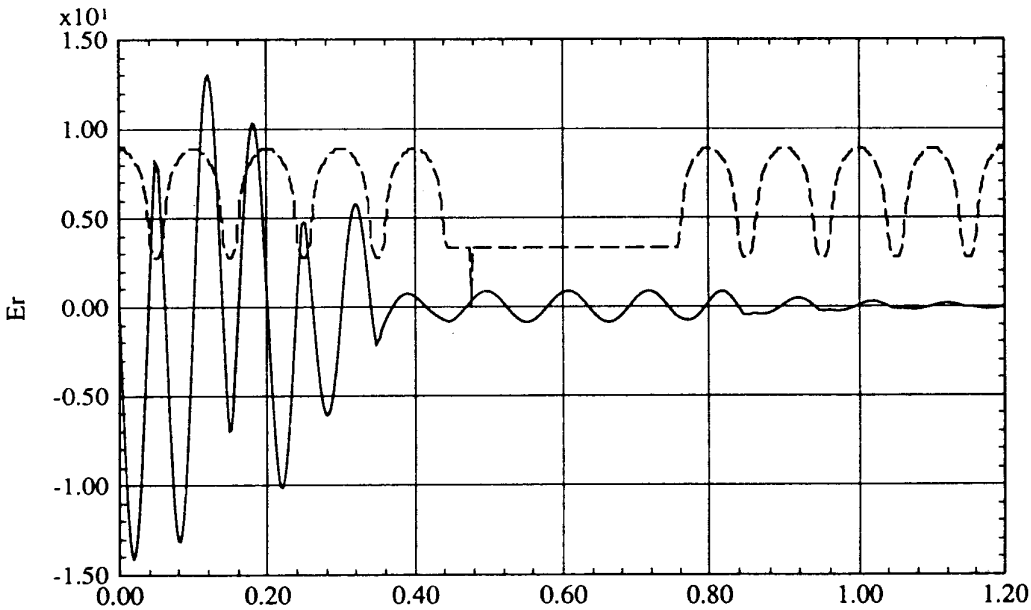

Figure 10 : radial electric field of the TM012 mode at 25mm from the beam axis along two 9-cell cavities, 3 half wavelengths away from one another, while the second cavity is slightly detuned (the arrow shows the HOM coupler location)

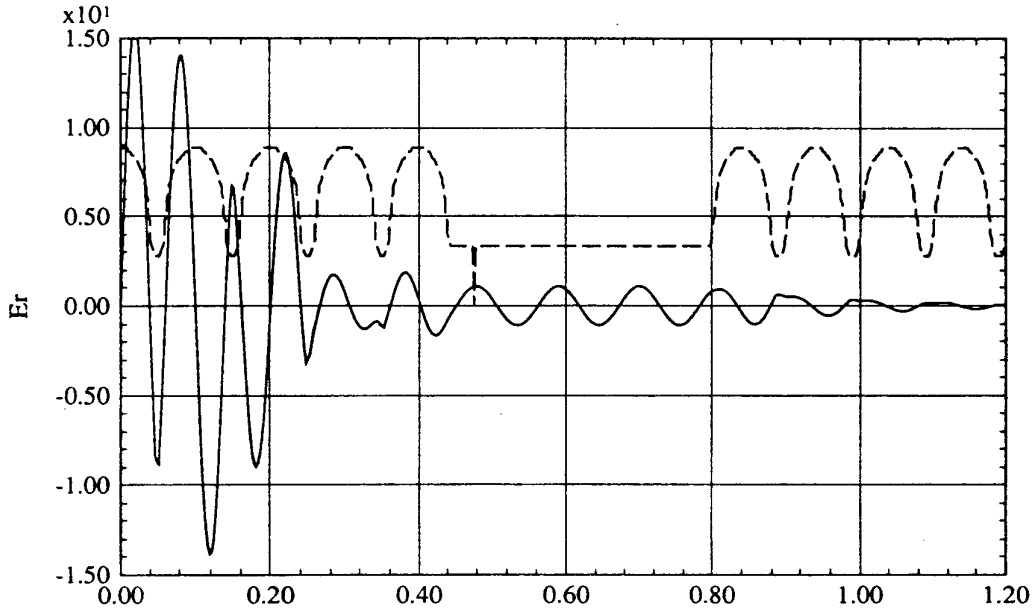

Figure 11 : radial electric field of the TM012 mode at 25mm from the beam axis along two 9-cell cavities, 3 half wavelengths plus 4 cm away from one another, while the second cavity is slightly detuned (the arrow shows the HOM coupler location)

5. Discussion

The small iris aperture cavity has a clear advantage in its gradient capability.because the peak surface electric field / accelerating field ratio is 40 % smaller. But what is now the overall refrigerator load for both structures ? The total power dissipated at low temperature includes losses from the accelerating mode, higher order mode power and the static heat leak. The cavity dissipation which depends on Q_0 will be higher for the large iris cavity but the HOM losses will be higher for the small iris cavity. On the other hand, if non superconducting parts are disposed in between 8-cavities modules at intermediate temperature, we are confident that at least 90 % of the HOM power above cut-off will dump there, so that only 10 % will be dissipated in helium. Figure 10 shows the cryogenic load versus Q_0 for both cavities without beam tube reduction for a typical set of parameters :

gradient	25 MV/m
number of particles / bunch	$5\ 10^{10}$
average collision frequency	8 kHz
bunchlength	2 mm
static losses	1 W/m

With beam tube reduction, about 0.1 W/m has to be added on both curves. The cryogenic load is clearly higher for the large iris cavity in case of high gradient. We conclude therefore that the small iris cavity is more advantageous both for its gradient capability and for the refrigerator load.

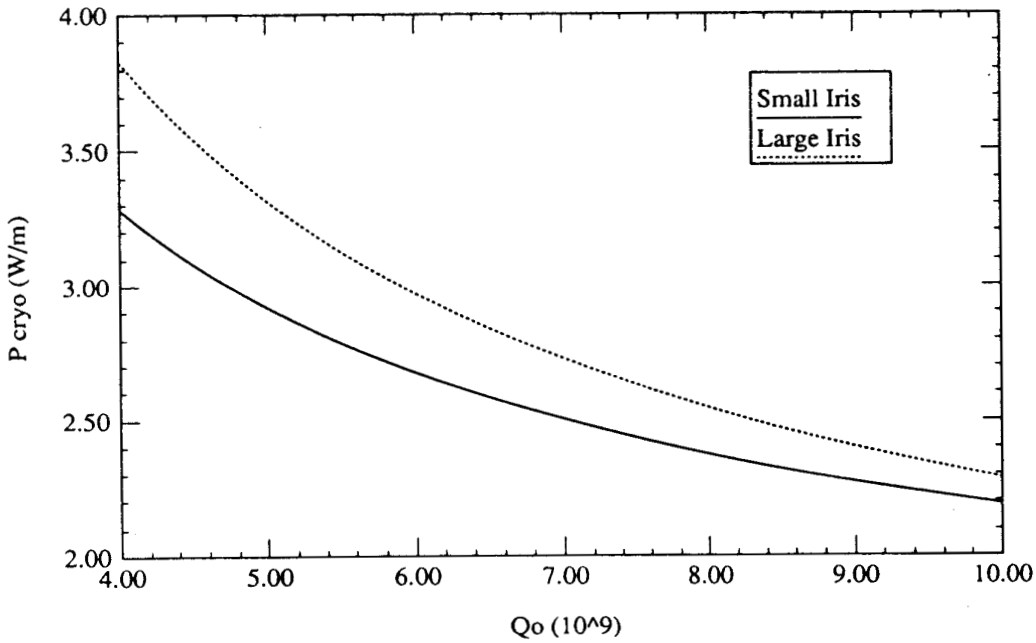

Figure 10 : Dissipated power in helium for small and large iris aperture cavities.

References

[1] Proc. of the 1st TESLA Workshop, Cornell U, Ithaca, NY, CLNS 90-1029 (1990)
[2] T. Weiland, Nucl. Inst. and Meth. 216, 329 (1983)
[3] A. Mosnier, in refs [1] "The trapped modes in a multicell SC cavity"
[4] T. Weiland, CERN-ISR-TH/80-45
[5] Y.H. Chin, CERN/LEP-TH/88-3
[6] R. Gluckstern, Proc. of the 1989 Part. Acc. Conf., Chicago, March 1989
[7] D.L. Rubin, Proc. of the 1989 Part Acc. Conf.,.Chicago, March 1989 K. Thompson in [1], P. 286
[8] E. Haebel, P. Marchand, J. Tückmantel, CERN/EF/RF 84-2 "An Improved Superconducting Cavity Design For LEP"
[9] E. Haebel, P. Marchand, J. Tuckmantel, CERN/EF/RF 84-1
[10] A. Mosnier, Proc. of the 4th Workshop on RF Supercond., Tsukuba, 1989
[11] D. Moffat and al., 1991 Part. Acc. Conf., San Francisco, May 1991 "Use of Ferrite-50 to strongly damp higher order modes"
[12] D. Proch, H. Heinrichs in [1], P. 605